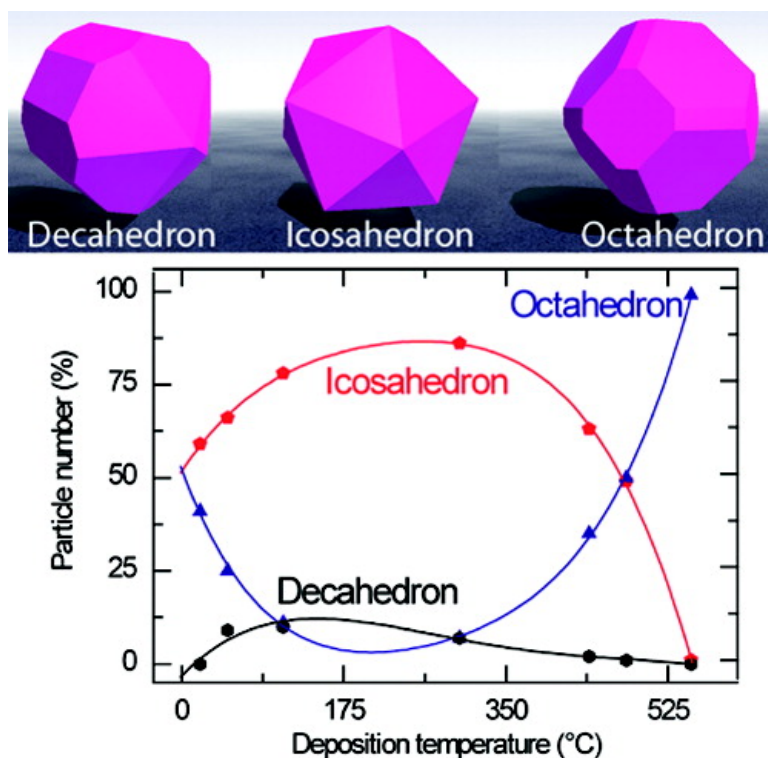


Temperature-Dependent Stability of Supported Five-Fold Twinned Copper Nanocrystals

Fabien Silly, and Martin R. Castell

ACS Nano, 2009, 3 (4), 901-906 • DOI: 10.1021/nn900059v • Publication Date (Web): 26 March 2009

Downloaded from <http://pubs.acs.org> on April 28, 2009



More About This Article

Additional resources and features associated with this article are available within the HTML version:

- Supporting Information
- Access to high resolution figures
- Links to articles and content related to this article
- Copyright permission to reproduce figures and/or text from this article



[View the Full Text HTML](#)



Temperature-Dependent Stability of Supported Five-Fold Twinned Copper Nanocrystals

Fabien Silly^{†,*,*} and Martin R. Castell^{†,*,*}

[†]Department of Materials, University of Oxford, Parks Road, Oxford OX1 3PH, U.K., and [‡]CEA-Saclay, SPCS/IRAMIS, F-91191 Gif-sur-Yvette, France

There is intense interest in supported metal clusters and nanocrystals because they possess optical and chemical properties that are not exhibited in the respective bulk metals.^{1–3} The properties are affected by the size, shape, and structure of the nanocrystals as well as their interaction with the substrate. Increases in cluster size can be readily achieved through ripening processes, but structural and shape changes are more difficult to control. One structure change that is possible for some face centered cubic (fcc) metals on the nanoscale is the transition between multiply twinned particles (MTPs) and single crystals.⁴ MTPs are created through interlocking fcc tetrahedra with twin boundaries between them. They adopt structures with five-fold symmetry and exhibit morphologies with an icosahedral or decahedral shape.^{5–8} These nanocrystals only have low energy surface facets and hence have a lower surface energy than their single crystal counterparts, but the tetrahedral segments in MTPs do not result in a perfectly space filling structure. This gives rise to internal strain in the nanocrystals, which grows rapidly with increasing size, so that the MTP morphology is only thermodynamically stable for small volumes.^{9–16} However, theoretical studies have shown that the MTP to single crystal stability transition is a function of temperature as well as volume.¹⁵ In this paper, we report on Cu nanocrystals grown on SrTiO₃(001). The investigation shows that the sample temperature during Cu deposition is a key factor in determining whether the nanocrystals adopt a MTP or fcc single crystal structure. We use the experimental data to determine the temperature-dependent stability regimes of the MTP and single crystal structures of Cu nanocrystals.

ABSTRACT The temperature-dependent structure transition of supported Cu nanocrystals on SrTiO₃(001)-(2 × 1) is investigated by scanning tunneling microscopy (STM). We experimentally determine the phase map of supported Cu icosahedral, decahedral, and truncated octahedral nanocrystal shapes as a function of substrate temperature during Cu deposition. We show that a supported nanocrystal of 8500 atoms at a nucleation temperature of 480 °C has the same probability of adopting an icosahedral or octahedral shape.

KEYWORDS: nanocrystal · phase diagram · icosahedron · octohedron · decahedron · oxide · scanning tunneling microscopy

There are a variety of studies where theoretical phase diagrams have been produced that show the stability regime for MTP structures (icosahedrons, decahedrons) and fcc single crystals (octahedrons) versus size and temperature.^{15,17,18} However, depending on which model is used, there are conflicting predictions for a certain range of cluster volumes. The Ajayan and Marks model,¹⁵ based on Gibbs free energy calculations, predicts a MTP to single crystal transition with increasing temperature at constant volume. The Kuo and Clancy model¹⁷ uses molecular dynamics simulations and predicts the transition to be from single crystal to MTP with increasing temperature. This discrepancy highlights the need for experimental data concerning the stability regime of MTPs. In addition, the existing models are for free clusters, whereas many applications use supported clusters or nanocrystals. The interface between the nanocrystal and the support may significantly influence the relative stabilities of the nanocrystal shapes.¹⁹

Here we report a scanning tunneling microscopy (STM) investigation of Cu clusters and nanocrystals grown on a (2 × 1) reconstructed SrTiO₃(001) substrate. The STM images show that sample temperature during Cu deposition is a key factor in determining whether nanocrystals adopt a MTP or fcc

*Address correspondence to
fabien.silly@cea.fr,
martin.castell@materials.ox.ac.uk.

Received for review January 15, 2009
and accepted March 09, 2009.

Published online March 26, 2009.
10.1021/nn900059v CCC: \$40.75

© 2009 American Chemical Society

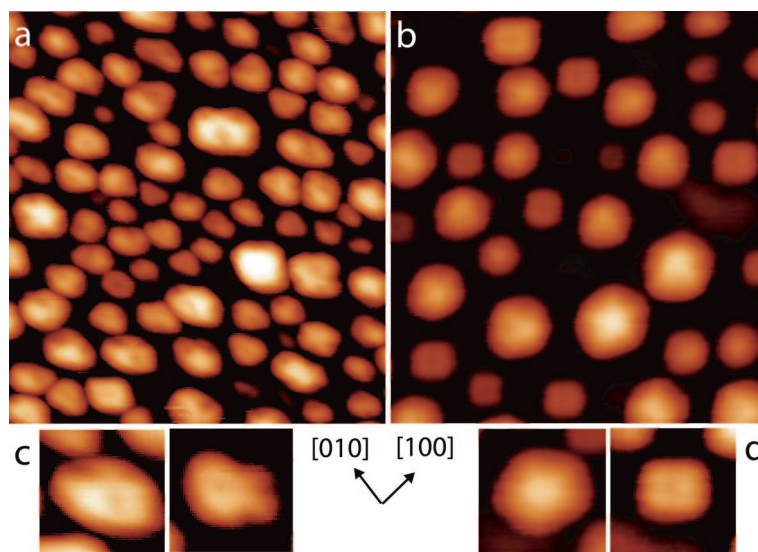


Figure 1. (a) Cu deposition onto a 110 °C SrTiO₃(001)-(2 × 1) substrate causes Cu cluster formation as shown in the STM image. (b) Cu deposition onto a room temperature substrate followed by a 560 °C anneal gives rise to truncated pyramid shaped nanocrystals and MTPs (images size = 37 × 41 nm²; $V_s = +4.0$ V, $I_t = 50$ pA). (c) Notched particles (8 × 8 nm²). (d) Icosahedron (9 × 9 nm²) and truncated pyramid shapes (7 × 7 nm²).

single crystal shape. We use the experimental data to determine the temperature-dependent phase map of the supported Cu nanocrystal structure on SrTiO₃(001)-(2 × 1), and we determine the transition point between the nanocrystal fcc and icosahedral shape.

RESULTS

Figure 1a shows the topography of the SrTiO₃(001) surface following Cu deposition at 110 °C. Cu forms distinct clusters, but they do not have a uniform shape or obvious crystallographic structure. However, a majority of these clusters possess 3 or 4 converging notches. Figure 1b shows the topography of the SrTiO₃(001) surface following Cu deposition on a substrate at room temperature followed by a 560 °C anneal for 1 h. The Cu forms new nanocrystals, which can be separated into two distinct shapes. One shape is that of a truncated pyramid with a square top surface and base. The second shape has five-fold symmetry, and the nanocrystals are either icosahedrons or Marks decahedrons, as illustrated in Figure 2. It should be noted that in Figure 1b the truncated pyramid nanocrystals are consistently smaller than the icosahedral nanocrystals.

The majority of the Cu nanocrystals with five-fold symmetry in Figure 1b have icosahedral shapes. Three high symmetry orientations for supported icosahedral nanocrystals are observed in our experiments (Figure 2a–c). Icosahedrons can be situated with the five-fold axis perpendicular to the substrate plane (point orientation, Figure 2a), with one tetrahedral face parallel to the substrate (face orientation, Figure 2b) or with only the topmost edge parallel to the substrate (edge orientation, Figure 2c). The main orientations observed for

the Marks decahedral nanocrystals are the point orientation (Figure 2d) and the side orientation (Figure 2e). The STM images of icosahedral and decahedral nanocrystals often have notches along facet edges as previously noticed on pentagonal small crystals.²⁰

Figure 3a shows the topography of the SrTiO₃(001) surface following Cu deposition on a substrate heated to 300 °C followed by a 1 h, 530 °C anneal. Under these nucleation conditions, Cu mainly forms icosahedra in the point orientation. For these nanocrystals, the ratio of the edge width (w) of the triangular facets to the height (h) of the icosahedral point is shown in Figure 3c. This ratio remains constant as a function of nanocrystal volume, implying that these icosahedral clusters have reached their equilibrium shape. The ratio is $w/h = 1.55 \pm 0.09$. As a guide to the eye, we have shown in Figure 3b a schematic illustration of the supported equilibrium shape of the icosahedral nanocrystal in the point orientation.

Figure 4 shows the topography of the SrTiO₃(001) surface following deposition of Cu on a substrate heated to 560 °C followed by a 1 h anneal at 560 °C. Less than 1% of the nanocrystals have icosahedral shapes. In Figure 4a, the majority of the Cu nanocrystals have a truncated pyramid shape with truncated edges as shown in the high-resolution STM image (Figure 4b). The predominant nanocrystal height was measured at 5.19 ± 0.56 nm. The side facets of the nanocrystals were measured at an angle of $54.4 \pm 1.5^\circ$ with respect to the substrate. These investigations show that the Cu nanocrystals have an fcc structure, which has a (001) top facet parallel to the substrate and four (111) side facets. In addition, (110) facets truncate the junctions where the (111) facets meet. The interface is therefore a (001) plane, and the interface crystallography is $(001)_{\text{Cu}} \parallel (001)_{\text{SrTiO}_3}$, $[100]_{\text{Cu}} \parallel [100]_{\text{SrTiO}_3}$. The ratio of the width (w) of the top square to the height (h) of the nanocrystal as a function of volume is shown in Figure 4d. The constant ratio of $w/h = 1.06 \pm 0.07$ implies that these nanocrystals have reached their equilibrium shape. As a guide to the eye, Figure 4c shows a schematic illustration of a supported nanocrystal calculated using the Wulff construction with the theoretically calculated fcc Cu surface energies ($\gamma_{001} = 2.166$ J/m², $\gamma_{111} = 1.952$ J/m², $\gamma_{110} = 2.237$ J/m²)²¹ and the experimentally determined w/h ratio from Figure 4d.

Figure 5a shows the measured proportions of icosahedral, decahedral, and fcc nanocrystal shapes as a function of substrate temperature during Cu deposition. Following deposition, all of the samples were annealed above 500 °C. The distribution shows that the proportion of icosahedral MTPs and nanocrystals at 20 °C is 59 and 41%, respectively. At 300 °C, the distribution

is 83 and 10%, and at 480 °C, it is 49 and 50%. We find that the percentage of Marks decahedral cluster shapes is always less than 10%, and that there is a similar trend with deposition temperature as for the icosahedra. Presumably, this similarity is because Marks decahedra and icosahedra are both MTPs. Figure 5b–e shows the histograms of icosahedral MTPs and truncated pyramid shaped fcc nanocrystals by volume nucleated at room temperature (rt) and 480 °C. It should be noted that the volume distribution of the two cluster types is similar at 480 °C (Figure 5c,d).

DISCUSSION

The formation of small nanocrystals with shapes that deviate from the single crystal Wulff shape can arise in fcc metals which exhibit low twin boundary energies and anisotropy of the surface facet energies. In a MTP, the surface energy is lowered to the detriment of an increase in internal strain. MTPs have a greater proportion of low energy $\{111\}$ facets than the equivalent fcc single crystals. For the equilibrium nanocrystal shape to be a MTP, therefore, depends on the internal strain being smaller than the reduction of total surface energy when compared with a single crystal. For supported nanocrystals, there are further factors that need to be taken into account, such as the interface and substrate surface energies and the epitaxial relationship between the MTP and the substrate. Nanocrystal phase diagrams have been calculated,^{15,17} which show the change in equilibrium shape as a function of size and temperature. These simulations can lead to conflicting predictions, and when a substrate is included in the calculations, the stability regions and morphological transition boundaries can be quite different from those of free nanocrystals.¹⁷

The experimental data shown in Figure 5a can be divided into two sections: from RT to 180 °C and from 180 to 560 °C. Nucleation at RT results in amorphous and polycrystalline Cu clusters, which increase their volume through ripening and turn into fcc nanocrystals or MTPs during the post deposition anneal at 560 °C. Increased nucleation temperatures from RT up to 180 °C cause a relative increase in MTP icosahedra. Presumably, this is because higher temperatures allow atomic ordering to be established from the early nanocrystal nucleation stage and MTPs are favored at small volumes. As nucleation temperatures are increased from 180 to 560 °C, we find that the entropy contribution has an increasingly significant influence on the relative stability of nanocrystal shapes, resulting in all nanocrystals being of fcc nanocrystal type at 560 °C. As expected, with increasing nucleation temperature, we also observe an upward shift in the nanocrystal population size. However, the size increase is not sufficient to explain the change in nanocrystal shapes, and we must therefore conclude that entropy is driving the shape changes. We find that at 480 °C the populations of fcc nanocrystals

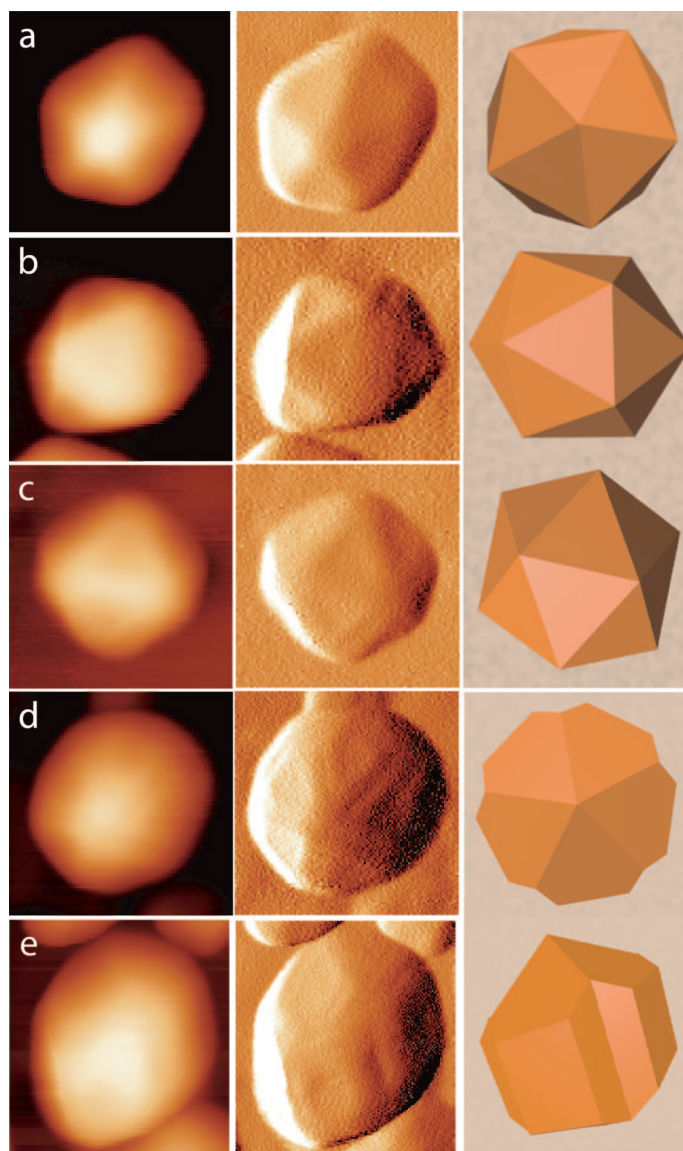


Figure 2. Icosahedral Cu nanocrystals in the (a) point orientation ($15 \times 15 \text{ nm}^2$), (b) face orientation ($12 \times 12 \text{ nm}^2$), and (c) edge orientation ($11 \times 11 \text{ nm}^2$). Marks decahedral nanocrystals in the (d) point orientation ($15 \times 15 \text{ nm}^2$) and (e) side orientation ($15 \times 16 \text{ nm}^2$). The top row shows topographic STM images ($V_s = +4.0 \text{ V}$, $I_t = 50 \text{ pA}$), the second row shows derivative images to accentuate the crystal faces, and the bottom row shows 3D models.

and MTP icosahedra are similar. Their size distributions are both centered on ~ 8500 atoms. Therefore, in the shape phase diagram, the point at 480 °C and ~ 8500 atoms is on the boundary of stability between the MTP icosahedron and the fcc nanocrystal shape.

The equilibrium shape of a Cu nanocrystal on a $\text{SrTiO}_3(001)$ substrate is determined by the surface energies of the Cu nanocrystal facets (γ_{hkl}), the interface energy between the Cu nanocrystal and the substrate (γ_i), and the surface energy of the substrate (γ_{STO}). The change in surface and interface energy between a bare substrate and one supporting a crystal is $E = \sum \gamma_{hkl} A_{hkl} + \gamma^* A_i$, where A_{hkl} are the Cu facet areas, A_i is the interface area, and γ^* is defined as $\gamma_i - \gamma_{\text{STO}}$.²² In the case of

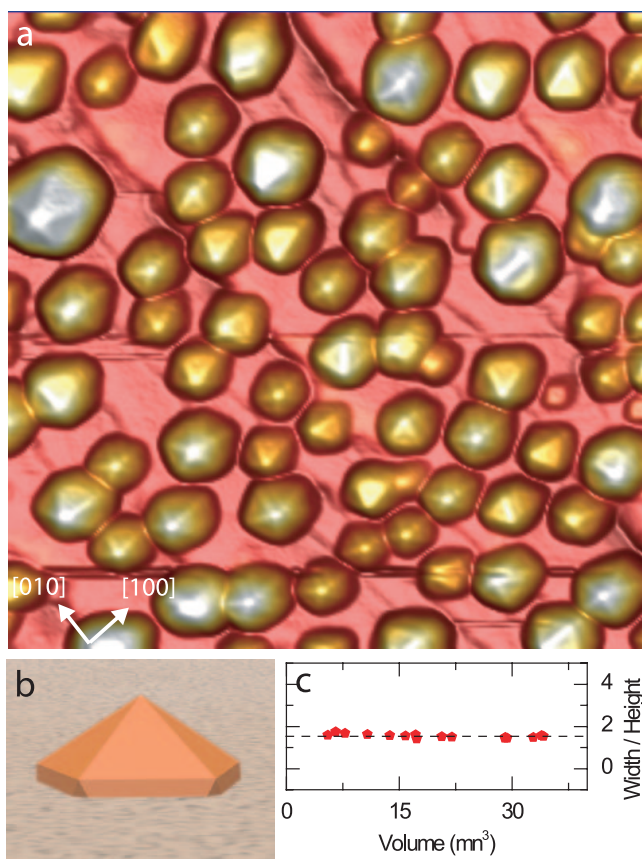


Figure 3. (a) Cu deposition onto a 300 °C SrTiO₃(001)-(2 × 1) substrate followed by a 1 h, 530 °C anneal gives rise to icosahedral shaped nanocrystals (70 × 70 nm²; $V_s = +4.0$ V, $I_t = 30$ pA). (b) Model of the supported icosahedral nanocrystal in the point orientation. The constant width to height ratio is shown in (c).

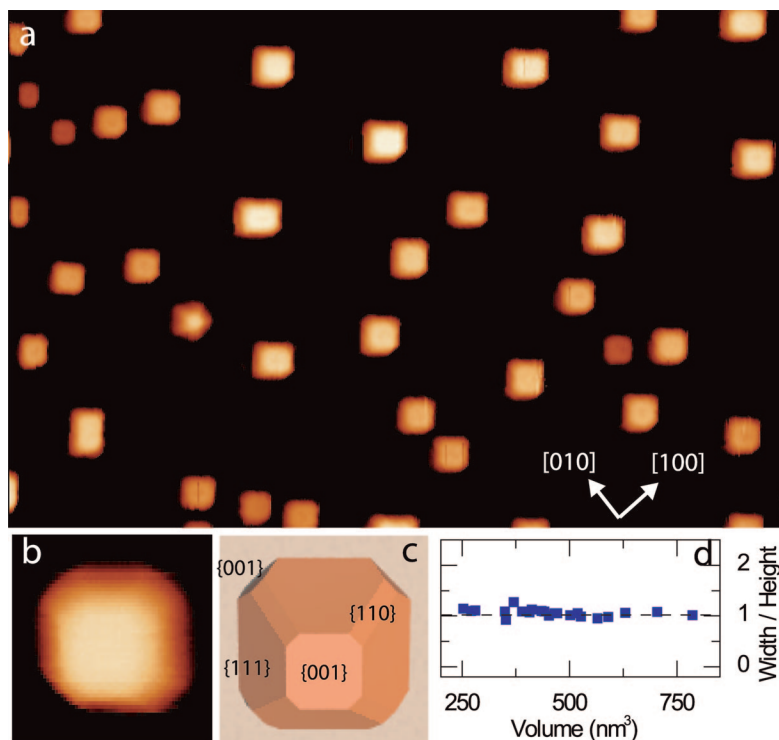


Figure 4. (a) Cu deposition onto a 560 °C SrTiO₃(001)-(2 × 1) substrate followed by a 560 °C anneal gives rise to truncated pyramid shaped nanocrystals as shown in the STM image (170 × 120 nm²; $V_s = +4.0$ V, $I_t = 30$ pA). (b) STM image of a nanocrystal ($V_s = +4.0$ V, $I_t = 30$ pA). (c) Three-dimensional model with the {111}, {110}, and {001} faces indicated. (d) Measured width to height ratio of the nanocrystals as a function of volume.

the fcc truncated octahedron shape, {111}, {001}, and {110} facets are present. Straightforward analysis *via* the modified Wulff construction²² results in the following equation for γ^* for the supported fcc octahedral (oct):

$$\gamma_{\text{oct}}^* = \left(\frac{w}{h}\right)^{-1} \sqrt{2}(\sqrt{3}\gamma_{111} - \gamma_{001}) - \gamma_{001} \quad (1)$$

In order to apply correctly the Wulff–Kashiev or Winterbottom theorem, it is necessary to be sure that the supported nanocrystals are fully relaxed. If the nanocrystal is only partially relaxed, the equilibrium shape is a function of the particle size.²³ As shown in Figure 4d, we did not observe changes in the nanocrystal shape with increasing volume, which suggests that the nanocrystals are unstrained.

In eq 1, we can substitute the w/h ratio from our experimentally determined values, and use the theoretically calculated fcc Cu surface energies of ref 21 ($\gamma_{001} = 2.166$ J/m², $\gamma_{111} = 1.952$ J/m²), which results in $\gamma_{\text{oct}}^* = (-0.545 \pm 0.107)$ J/m². We can estimate the adhesion energy of the truncated octahedron shape γ_{adh} of Cu on SrTiO₃(001)-(2 × 1), which is defined by $\gamma_{\text{adh}} = \gamma_{001} - \gamma_i + \gamma_{\text{STO}} = \gamma_{001} - \gamma_{\text{oct}}^*$. This results in $\gamma_{\text{adh}} = (2.711 \pm 0.107)$ J/m². The energy of the nanocrystals can also be written as $E = \alpha_{\text{shape}} V^{2/3}$, where α_{shape} depends on the nanocrystal shape, the facet energies, and γ^* . We can calculate $\alpha_{\text{oct}} \sim 7.7$ J/m² for the equilibrium octahedron shape by using the fcc facet surface energies²¹ and γ_{oct}^* as demonstrated in ref 19. However, in the current calculation, we also include the effect of the {110} facets.

As mentioned previously, the nanocrystal populations nucleated at 480 °C with a size of ~ 100 nm³ are similar in number and size for octahedra and icosahedra. This indicates a size and temperature regime where the differently shaped nanocrystals have a similar surface and interface energy of $\sim 166 \times 10^{-18}$ J.

For unsupported Cu nanocrystals, theoretical studies at 0 K predict that for very small volumes up to 1000 atoms the icosahedron is the most stable structure, followed by the decahedron up to 40 000 atoms. Above this volume, the fcc octahedron is the most stable shape.¹⁴ Other modeling studies that include entropic contributions to the nanocrystal energy also predict significant regions of stability for decahedrons.^{15,16} In our study, decahedra are rarely seen (less than 12% of the nanocrystals), which is probably due to the influence of the substrate. The substrate also influences the stability boundary between MTPs and fcc crystals. In unsupported MTPs, much of the strain is concentrated toward the center of the particle.^{14,24} As the Wulff point of

the Cu nanocrystals in our study lies below the substrate surface, the high strain region that is normally present in unsupported nanocrystals is not present in our supported nanocrystals. This effect allows supported MTPs to grow larger in volume than their unsupported counterparts.

CONCLUSION

In summary, we have investigated the structure transition of Cu nanocrystals on SrTiO₃(001)-(2 × 1). Our results show that Cu crystallizes into fcc nanocrystals and five-fold MTPs depending on the size of the nanocrystals and the substrate temperature during nucleation. These results demonstrate experimentally that, by varying the entropic contribution to the energy of supported nanoparticles, distributions with specific relative abundances of MTPs and fcc single crystals can be achieved. These Cu nanocrystals on SrTiO₃(001) are model candidates to investigate the structure and

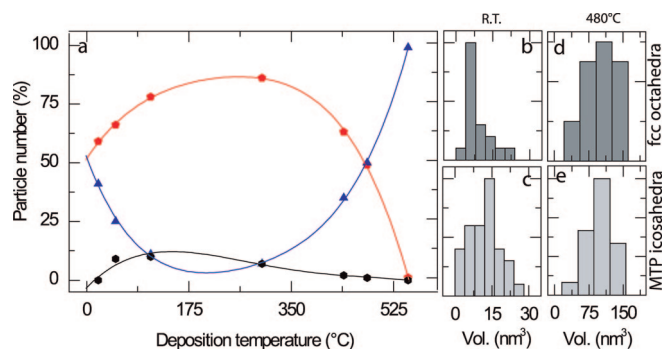


Figure 5. (a) Evolution of the proportion of Cu nanocrystal shapes as a function of nucleation temperature. Red pentagon points represent the MTP icosahedral shapes, blue triangular points represent fcc nanocrystals, and black hexagonal points represent MTP Marks decahedron shapes. Best fit lines have been drawn through the data points. (b–e) Volume distributions of Cu nanocrystals nucleated at room temperature and at 480 °C for icosahedral shapes (c,e) and fcc nanocrystals (b,d), respectively.

shape-dependent electronic and optical properties of metal nanocrystals.

EXPERIMENTAL SECTION

As a substrate for Cu nanocrystal growth, we use SrTiO₃(001). This surface presents a multitude of different reconstructions depending on sample preparation.²⁵ These reconstructions can be used to control the growth of nanocrystals.¹⁹ We use SrTiO₃ crystals doped with 0.5% (weight) Nb, supplied by PI-KEM, U.K. SrTiO₃(001)-(2 × 1) reconstructed surfaces were prepared by argon ion sputtering and subsequent annealing in UHV at 600 °C for 9 h. The (2 × 1) surface reconstruction was imaged by STM and confirmed by low-energy electron diffraction (LEED). We deposited Cu from an e-beam evaporator (Oxford Applied Research EGN4) using 99.99% pure Cu rods supplied by Goodfellow, U.K. Our STM is manufactured by JEOL (JSTM 4500s) and operates in UHV (10⁻⁸ Pa). We used etched W tips to image the samples at room temperature with a bias voltage applied to the sample. STM images have been processed and analyzed with FabViewer.²⁶

Acknowledgment. The authors would like to thank the Royal Society and DSTL for funding, and Chris Spencer (JEOL U.K.) for valuable technical support.

REFERENCES AND NOTES

- Henry, C. R. Morphology of Supported Nanoparticles. *Prog. Surf. Sci.* **2005**, *80*, 92–116.
- Campbell, C. T. Ultrathin Metal Films and Particles on Oxide Surfaces: Structural, Electronic and Chemisorptive Properties. *Surf. Sci. Rep.* **1997**, *27*, 1–111.
- Myroshnychenko, V.; Carbo-Argibay, E.; Pastoriza-Santos, I.; Perez-Juste, J.; Liz-Marzan, L. M.; Javier Garcia de Abajo, F. Modeling the Optical Response of Highly Faceted Metal Nanoparticles with a Fully 3D Boundary Element Method. *Adv. Mater.* **2008**, *20*, 4288–4293.
- Xiong, Y.; Xia, Y. Shape-Controlled Synthesis of Metal Nanostructures: The Case of Palladium. *Adv. Mater.* **2007**, *19*, 3385–3391.
- Marks, L. D. Experimental Studies of Small Particle Structures. *Rep. Prog. Phys.* **1994**, *57*, 603–649.
- Silly, F.; Castell, M. R. Growth of Ag Icosahedral Nanocrystals on a SrTiO₃(001) Support. *Appl. Phys. Lett.* **2005**, *87*, 213107.
- Sanchez-Iglesias, A.; Pastoriza-Santos, I.; Perez-Juste, J.; Rodriguez-Gonzalez, B.; Garcia de Abajo, F. J.; Liz-Marzan, L. M. Synthesis and Optical Properties of Gold Nanodecahedra with Size Control. *Adv. Mater.* **2006**, *18*, 2529–2534.
- Zhang, W.; Liu, Y.; Cao, R.; Li, Z.; Zhang, Y.; Tang, Y.; Fan, K. Synergy between Crystal Strain and Surface Energy in Morphological Evolution of Five-Fold-Twinned Silver Crystals. *J. Am. Chem. Soc.* **2008**, *130*, 15581–15588.
- Howie, A.; Marks, L. D. Elastic Strains and the Energy-Balance for Multiply Twinned Particles. *Philos. Mag. A* **1984**, *49*, 95–109.
- Ino, S. Stability of Multiply-Twinned Particles. *J. Phys. Soc. Jpn.* **1969**, *27*, 941–953.
- Uppenbrink, J.; Wales, D. J. Structure and Energetics of Model Metal Clusters. *J. Chem. Phys.* **1992**, *96*, 8520–8534.
- Valkealahti, S.; Manninen, M. Instability of Cuboctahedral Copper Clusters. *Phys. Rev. B* **1992**, *45*, 9459–9462.
- Cleveland, C. L.; Landman, U. The Energetics and Structure of Nickel Clusters: Size Dependence. *J. Chem. Phys.* **1991**, *94*, 7376–7396.
- Mottet, C.; Goniakowski, J.; Baletto, F.; Ferrando, R.; Treglia, G. Modeling Free and Supported Metallic Nanoclusters: Structure and Dynamics. *Phase Transitions* **2004**, *77*, 101–113.
- Ajayan, P. M.; Marks, L. D. Quasimelting and Phases of Small Particles. *Phys. Rev. Lett.* **1988**, *60*, 585–587.
- Reinhard, D.; Hall, B. D.; Ugarte, D.; Monot, R. Unsupported Nanometer-Sized Copper Clusters Studied by Electron Diffraction and Molecular Dynamics. *Phys. Rev. B* **1998**, *58*, 4917–4925.
- Kuo, C.-L.; Clancy, P. Melting and Freezing Characteristics and Structural Properties of Supported and Unsupported Gold Nanoclusters. *J. Phys. Chem. B* **2005**, *109*, 13743–13754.
- Doye, J. P. K.; Calvo, F. Entropic Effects on the Size Dependence of Cluster Structure. *Phys. Rev. Lett.* **2001**, *86*, 3570–3573.
- (a) Silly, F.; Castell, M. R. Selecting the Shape of Supported Metal Nanocrystals: Pd Huts, Hexagons, or Pyramids on SrTiO₃(001). *Phys. Rev. Lett.* **2005**, *94*, 046103. (b) Silly, F.; Castell, M. R. Bimodal Growth of Au on SrTiO₃(001). *Phys. Rev. Lett.* **2006**, *96*, 086104.
- Marks, L. D. Surface-Structure and Energetics of Multiply Twinned Particles. *Philos. Mag. A* **1984**, *49*, 81–93.
- Vitos, L.; Ruban, A. V.; Skriver, H. L.; Kollar, J. The Surface Energy of Metals. *Surf. Sci.* **1998**, *411*, 186–202.
- Winterbottom, W. L. Equilibrium Shape of a Small Particle in Contact with a Foreign Substrate. *Acta Metall.* **1967**, *15*, 303–310.

23. Müller, P.; Kern, R. Equilibrium Nano-Shape Changes Induced by Epitaxial Stress (Generalised Wulff-Kaisewitz Theorem). *Surf. Sci.* **2000**, *457*, 229–253.
24. Mottet, C.; Rossi, G.; Baletto, F.; Ferrando, R. Single Impurity Effect on the Melting of Nanoclusters. *Phys. Rev. Lett.* **2005**, *95*, 035501.
25. (a) Silly, F.; Newell, D. T.; Castell, M. R. SrTiO₃(001) Reconstructions: the (2 × 2) to c(4 × 4) Transition. *Surf. Sci.* **2006**, *600*, L219–L223. (b) Castell, M. R. Scanning Tunneling Microscopy of Reconstructions on the SrTiO₃(001) Surface. *Surf. Sci.* **2002**, *505*, 1–13. (c) Newell, D. T.; Harrison, A.; Silly, F.; Castell, M. R. SrTiO₃(001)-(√5 × √5)-R26.6° Reconstruction: A Surface Resulting from Phase Separation in a Reducing Environment. *Phys. Rev. B* **2007**, *75*, 205429. (d) Silly, F.; Castell, M. R. Encapsulated Pd Nanocrystals Supported by Nanoline-Structured SrTiO₃(001). *J. Phys. Chem. C* **2005**, *109*, 12316–12319.
26. Silly, F. FabViewer, <http://dr-silly.atpspace.com/>.